ISSN 1070-3284, Russian Journal of Coordination Chemistry, 2023, Vol. 49, No. 12, pp. 822–829. © Pleiades Publishing, Ltd., 2023.
Russian Text © The Author(s), 2023, published in Koordinatsionnaya Khimiya, 2023, Vol. 49, No. 12, pp. 782–789.

Low-Temperature Behavior of the Heat Capacity and Photoluminescence of the Binuclear Pivalate Complex $[Eu_2(Bath)_2(Piv)_6]$

I. G. Fomina[a], *, A. V. Tyurin[a], Yu. S. Zavorotnyi[b], and I. L. Eremenko[a]

[a] *Kurnakov Institute of General and Inorganic Chemistry, Russian Academy of Sciences, Moscow, Russia*
[b] *Skobeltsyn Institute of Nuclear Physics, M.V. Lomonosov Moscow State University, Moscow, Russia*
**e-mail: fomina@igic.ras.ru*

Received July 4, 2023; revised July 11, 2023; accepted July 12, 2023

Abstract—The low-temperature behavior of the heat capacity and photoluminescence of the earlier structurally characterized binuclear pivalate complex $[Eu_2(Bath)_2(Piv)_6]$ (monoclinic crystal system, $I2/a$) (**I**), where Bath = 4,7-diphenyl-1,10-phenanthroline, Piv = $(CH_3)_3CCO_2^-$, is studied. The temperature dependence of the heat capacity in a temperature range of 5.96–302.88 K is measured by adiabatic calorimetry, and the thermodynamic functions $C_p^\circ(T)$, $S^\circ(T)$, $\Phi^\circ(T)$, and $H^\circ(T) - H^\circ(0)$ are calculated. The absence of low-temperature phase transitions in complex **I** is shown. In a temperature range of 98–295 K, complex **I** demonstrates a high temperature stability of the integral photoluminescence intensity of the ${}^5D_0$–${}^7F_j$ (j = 0–6) transitions of the Eu^{3+} ion.

Keywords: europium carboxylate, 4,7-diphenyl-1,10-phenanthroline, adiabatic calorimetry, photoluminescence

DOI: 10.1134/S107032842360105X

INTRODUCTION

Molecular lanthanide complexes with organic ligands have unique physicochemical properties and attract significant interest due to high prospects of their practical use as functional components of innovative materials in diverse fields of optics, magnetism, sorption, sensorics, etc. [1–4]. One of the most important physical properties of coordination lanthanide compounds with organic ligands is narrow-band (fullwidth at half of maximum, FWHM ~10 nm) photoluminescence (PL) in the visible or near-IR spectral range, whose specific mechanism provides high quantum yields. At present, serious attention is given to studying optical properties of the molecular Eu^{3+} complexes due to their possible practical use as light conversion molecular devices (LCMD). These devices can find use, for example, as functional components of light-emitting composite materials, optical sensors, luminescent labels for bioanalytical applications, etc. [1, 5–8]. Numerous Eu^{3+} complexes with organic ligands were studied in rather detail, but an absolute quantum yield of 40–60% is still rare for Eu^{3+} coordination compounds. According to the commonly accepted concept of sensitized luminescence, in lanthanide complexes with organic ligands the excitation energy is absorbed by the chromophoric groups of the organic ligand, then is transferred from its π^* or n^* levels to the corresponding closely lying 4f levels of the Ln^{3+} ion ($S_0 \rightarrow S_1 \rightarrow T_1 \rightarrow Ln^*$, “antenna” effect) inside the molecule, and is emitted (due to f–f transitions) as a set of PL bands characteristics of this lanthanide ion [2, 8–10]. The excitation energy transfer $S_0 \rightarrow S_1 \rightarrow Ln^*$ occurs in some cases [11–15]. The PL intensity of the Ln^{3+} complexes is determined, on the one hand, by the excitation energy transfer from the π^* or n^* levels of the ligand to the resonance level of the lanthanide ion and, on the other hand, by nonradiative relaxation channels of the excited levels of the ligands and excited levels of the lanthanide ion, the existence of which is caused by the ligand nature, influence of the temperature and solvent, and others factors. The character of the excitation energy transfer from the ligand levels to the excited levels of the lanthanide ion is activation: the efficiency of excitation energy transfer increases with increasing temperature. The nonradiative relaxation channels are also activated with temperature. As a result, depending on the activation energies for each channel, both a decrease or an increase in the PL intensity and a more complicated dependence, sign-variable with respect to the first derivative of temperature, can be observed in a specified temperature range.

We have recently reported on a possibility of the synthesis of binuclear pivalates $[Eu_2(Bath)_2(Piv)_6]\cdot x$Solv (where Bath = 4,7-diphenyl-1,10-phenanthroline; Piv = $(CH_3)_3CCO_2^-$; Solv = EtOH, H_2O; x = 0–2) having the same composition of the internal sphere of the lanthanide ion and different molecular and crystal structures and on their thermal behavior studied by differential scanning calorimetry and thermogravimetry and PL properties [16, 17]. In particular, the differences in the molecular geometries of the Eu^{3+} ions in the complexes $[Eu_2(Bath)_2(Piv)_6]\cdot x$Solv were shown to induce no decrease in a high luminescence intensity of the Eu^{3+} ion in these compounds at 300 K [16]. In this work, in order to establish the presence or absence of possible II order phase transitions capable of affecting luminescence, the temperature dependence of the heat capacity of the complex $[Eu_2(Bath)_2(Piv)_6]$ (monoclinic, $I2/a$) (**I**) in a temperature range of 5.96–302.88 K was studied by adiabatic calorimetry. In addition, the temperature stability of the integral PL intensity of the Eu^{3+} ion $^5D_0$–^7F_j (j = 0–6) transitions in a temperature range of 98–295 K was studied for complex **I** and complexes $[Eu_2(Phen)_2(Piv)_6]$ (**II**), where Phen = 1,10-phenanthroline and $[Eu_2(Bpy)_2(Piv)_6]$ (**III**), where Bpy = 2,2'-bipyridine, exhibiting significant intensity and monochromaticity of PL at 300 K [18, 19].

EXPERIMENTAL

Binuclear pivalates **I**–**III** were synthesized using known procedures [16, 18]. The following reagents were used in the synthesis: HPiv (≥98%, Acros Organics), $Eu(OAc)_3\cdot xH_2O$ (99.99%, Alfa Aesar), Bath (99%, Chempur), Bpy (99%, Alfa Aesar), Phen (99%, Alfa Aesar), and EtOH (96%). The H_2O content in $Eu(OAc)_3\cdot xH_2O$ was determined by thermogravimetry. Phase X-ray diffraction (XRD) analysis of $[Eu_2(Bath)_2(Piv)_6]$ was carried out on a D8 ADVANCE X-ray diffractometer (CuK_α, Ni filter, LYNXEYE detector).

The heat capacity was measured by vacuum adiabatic calorimetry on a BKT-3 low-temperature calorimetric setup (AOZT TERMIS, Mendeleevo, Moscow region). The measurements were carried out in the automated mode using a system consisting a computer and an Aksamit-9 control unit for analog data processing. A sample was placed in a thin-walled titanium cylindrical container with an inner volume of 1 cm^3. The container was filled in a special chamber in a helium atmosphere at a pressure of 10 kPa. The calorimeter temperature was measured with a resistance iron–rhodium thermometer. The sensitivity of the temperature measuring system was 10^{-3} K, and the sensitivity of the analog-digital converter was 0.1 μV. To check the measurement procedure, the heat capacity of the standard sample of benzoic acid (class K-2) was determined in a temperature range of 5–350 K. The measurements show that the accuracy of heat capacity measurement is ±2% at helium temperatures, decreases to ±0.4% with increasing temperature to 40 K, and amounts to ±0.2% in a range of 40–350 K. The sample was weighed for measurements with an accuracy of 2×10^{-5}. A weighed sample of the substance for measurements was 0.23413 g, and the molecular weight was accepted to be 1575.42 g/mol. The design and principle of setup operating and measurement procedure were described in detail [20, 21].

The experimental values of heat capacity for complex **I** measured in a temperature range of 5.96–302.88 K are listed in Table 1. The experimental data obtained by adiabatic calorimetry were smoothened using Eq. (1) [22], the coefficients of which are given in Table 2.

$$C_p(T) = \sum_0^5 A_j U^j, \quad U = \ln\left(\frac{T}{400}\right), \tag{1}$$

where A and j are the coefficient and exponent of the logarithmic polynomial dependence of the heat capacity, respectively. Equation (1) was also used for the calculation of the entropy $S°(T)$, change in enthalpy $H°(T)$–$H°(0)$, and reduced Gibbs energy $\Phi°(T)$ of complex **I**. The thermodynamic properties of complex **I** are given in Table 3.

The PL excitation was induced by an UV light diode with a wavelength of 340 nm, and the FWHM of 11 nm. The compounds were grinded, sealed in a glass capillary, and placed in optically transparent Dewar flask above the level of boiling liquid nitrogen. The PL spectra of the compounds were recorded during natural heating of the sample in a temperature range of 98–295 K on an Ocean Optics Maya2000 Pro spectrometer, and the BS-8 color glass filter was placed between the spectrophotometer and sample. The temperature was measured with a K type thermocouple mounted in the Dewar flask near the sample. The thermocouple voltage was measured by a microvoltmeter and recalculated to the temperature taking into account the cold junction temperature (microvoltmeter terminals at room temperature) using ITS-90 tables [23]. The obtained spectra were corrected to the spectral sensitivity of the apparatus and reduced to the quantum spectral density by energies (frequencies). To estimate the PL intensity of the Eu^{3+} ion caused by the brightest bands of transitions from the $^5D_0$ level, integration in a wavelength range of 564–880 nm corresponding to the luminescence bands of the $^5D_0$–^7F_j (j = 0–6) transitions was performed in each measured spectrum. The lifetimes of the $^5D_0$ level of the Eu^{3+} ion (τ) for the complexes at 98 K were calculated using the Mott model according to which the lifetime of the excited level τ is determined from the equation [24]

Table 1. Experimental heat capacities for complex **I** (in J K^{-1} mol^{-1})

T, K	C_p	T, K	C_p	T, K	C_p	T, K	C_p
Series 1		181.85	1020	7.92	20.0	49.15	339.0
79.20	507.4	185.15	1037	8.54	24.1	50.77	353.7
82.04	527.9	188.45	1054	9.20	27.6	52.39	368.8
84.09	531.9	191.76	1070	9.87	32.1	54.02	386.3
86.15	541.3	195.06	1087	10.56	36.43	55.64	406.7
88.20	566.7	198.35	1102	11.25	41.32	57.27	424.6
90.26	574.2	202.06	1125	11.96	47.79	58.90	425.9
Series 2		206.17	1146	12.67	55.90	60.55	436.6
95.05	584.4	210.28	1168	13.41	61.24	62.19	440.4
97.93	607.9	214.38	1193	14.16	66.06	63.84	439.0
99.99	618.0	218.47	1217	14.92	72.62	65.49	440.5
102.66	629.3	222.56	1242	15.69	77.24	67.14	446.4
105.94	644.8	226.64	1266	16.46	83.09	68.79	451.1
109.22	653.3	230.67	1291	17.24	88.09	70.44	456.9
112.51	668.9	234.75	1316	18.05	95.13	72.33	460.0
115.79	685.1	238.86	1341	18.83	100.4	74.39	469.4
119.08	700.0	242.93	1367	19.61	107.6	76.45	481.2
122.38	715.2	246.99	1391	20.88	125.4	Series 4	
125.67	730.6	251.04	1416	22.37	136.9	82.52	519.5
128.97	745.9	255.08	1441	23.88	149.9	85.40	531.7
132.26	762.5	259.10	1465	25.41	158.1	87.48	555.5
135.57	778.4	263.03	1487	26.94	172.1	89.55	567.2
138.87	794.5	267.04	1514	28.49	187.7	91.63	576.0
142.17	811.7	271.03	1539	30.04	206.8	93.71	584.2
145.48	829.6	275.01	1564	31.61	215.3	95.79	591.5
148.79	846.1	278.98	1588	33.19	225.4	97.87	601.7
152.09	863.7	282.89	1612	34.76	231.0	99.95	612.6
155.40	880.8	286.83	1637	36.34	247.6	102.65	623.8
158.70	897.7	290.75	1661	37.90	262.8	105.96	640.3
162.01	915.0	294.64	1684	39.49	272.8	109.27	656.0
165.31	934.4	298.53	1708	41.08	282.8	112.59	671.3
168.62	950.8	302.88	1740	42.68	292.5	115.91	687.0
171.93	967.7	Series 3		44.28	302.2		
175.23	986.0	5.96	4.83	45.92	314.0		
178.54	1002	7.37	15.7	47.53	326.4		

$$\tau = \left(k_R + k_0 e^{\frac{-E_A}{kT}} \right)^{-1}, \qquad (2)$$

where k_R is the radiative relaxation probability (6.7 ms)$^{-1}$ for the $^5D_0$ level of the Eu^{3+} ion [25]; $k_0 e^{\frac{-E_A}{kT}}$ is the nonradiative relaxation probability; T is the Kel-

Table 2. Coefficients in Eq. (1) (in J K^{-1} mol^{-1})

j	A_j
0	0.24187743 × 10^4
1	0.293056027 × 10^4
2	0.19822891 × 10^4
3	0.771613903 × 10^3
4	0.151844376 × 10^3
5	0.116113962 × 10^2

Table 3. Thermodynamic properties of complex **I**

T, K	$C_p^\circ(T)$ J K^{-1} mol^{-1}	$S^\circ(T)$ J K^{-1} mol^{-1}	$H^\circ(T) - H^\circ(0)$ J mol^{-1}	$\Phi^\circ(T) - \Phi^\circ(0)$ J K^{-1} mol^{-1}
10	35.71	12.84	96.17	3.218
20	112.7	59.73	816.9	18.88
25	156.7	89.59	1490	29.98
30	199.5	122.0	2381	42.58
35	239.9	155.8	3481	56.33
40	277.7	190.3	4776	70.91
45	313.0	225.1	6254	86.11
50	346.0	259.8	7902	101.7
60	406.6	328.3	11670	133.8
70	461.9	395.2	16020	166.3
80	513.6	460.3	20900	199.0
90	563.1	523.6	26280	231.6
100	611.4	585.5	32150	264.0
110	659.2	646.0	38510	295.9
120	706.9	705.4	45340	327.6
130	755.1	763.9	52650	358.9
140	803.8	821.6	60440	389.9
150	853.3	878.8	68720	420.6
160	903.8	935.4	77510	451.0
170	955.2	991.8	86800	481.2
180	1008	1048	96620	511.0
190	1061	1104	107000	540.5
200	1116	1160	117900	570.1
210	1172	1215	129300	599.7
220	1229	1271	141300	628.9
230	1287	1327	153900	658.0
240	1346	1383	167000	687.3
250	1406	1439	180800	716.1
260	1468	1496	195200	744.8
270	1530	1552	210200	773.7
280	1593	1609	225800	802.6
290	1657	1666	242000	831.5
298.15	1710	1713	255700	855.1
300	1722	1723	258900	860.3

vin temperature; E_A and k_0 are the activation energy of the channel and initial probability of activation, respectively; and k is the Boltzmann constant. The lifetimes of the $^5D_0$ level of the Eu^{3+} ion (τ) for the corresponding europium complexes at 295 and 77 K obtained earlier [19] were used in the calculation. The calculated lifetimes τ for complexes **I**, **II**, and **III** at 98 K were 1.77, 1.57, and 1.53 ms, respectively.

RESULTS AND DISCUSSION

In the structurally characterized binuclear complexes $[Eu_2(Bath)_2(Piv)_6]\cdot x$Solv (where Solv = H_2O, EtOH; x = 0–2) having the same composition of the internal sphere of the metal ion, the central fragment Ln_2Piv_4 has two structural types: $Ln_2(\mu_2\text{-Piv-}\kappa^2O,O')_4$ (**A**) and $Ln_2(\mu_2\text{-Piv-}\kappa^2O,O')_2(\mu_2\text{-Piv-}\kappa^2O,O,O')_2$ (**B**) (Scheme 1).

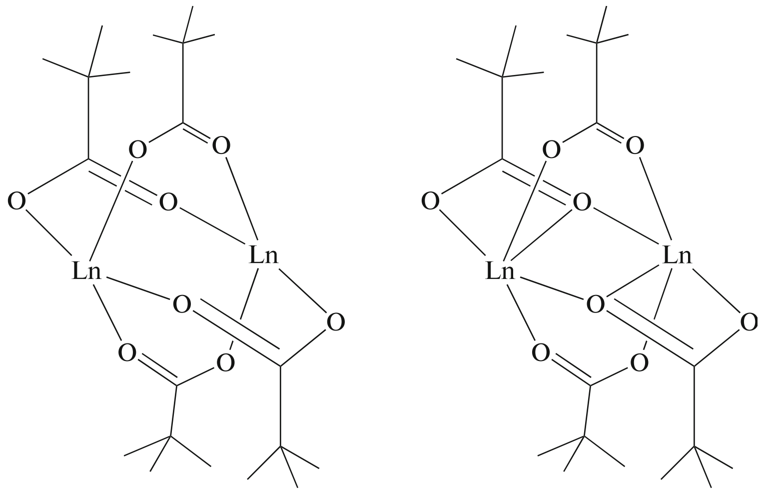

A **B**

Scheme 1.

The Ln_2Piv_4 central fragment has the structural type $Ln_2(\mu_2\text{-Piv-}\kappa^2O,O')_4$ (**A**, Scheme 1) in carboxylates $[Eu_2(Bath)_2(Piv)_6]\cdot xH_2O$, where $x = 0$ and 0.75 (monoclinic, *I*2/*a*), $[Eu_2(Bath)_2(Piv)_6]$ (monoclinic, $P2_1$), and $[Eu_2(Bath)_2(Piv)_6]\cdot x$EtOH, where $x = 0$ and 1.5 (monoclinic, *C*2/*c*) as in dimers $[Ln_2(HPiv)_6(Piv)_6]\cdot$HPiv, where Ln = La, Sm, Eu, Gd, and Tb [13, 16, 18, 19, 26, 27]. The coordination environment of each metallocenter (coordination number 8) is supplemented by ligands Piv-κ^2O,O' and Bath-κ^2N,N' or Piv-κ^1O and HPiv-κ^1O, respectively. The Ln_2Piv_4 central fragment has the structural type $Ln_2(\mu_2\text{-Piv-}\kappa^2O,O')_2(\mu_2\text{-Piv-}\kappa^2O,O,O')_2$ (**B**, Scheme 1) in pivalate $[Eu_2(Bath)_2(Piv)_6]\cdot 2$EtOH (triclinic, $P\bar{1}$) and dimers $[Ln_2L_2(Piv)_6]$, where Ln = Sm, Eu, Gd, Tb, and Er; L = Phen or Bpy [10, 16, 18, 19]. The coordination environment of each metallocenter (coordination number 9) is supplemented by ligands Piv-κ^2O,O' and Bath-κ^2N,N' or Phen-κ^2N,N' and Bpy-κ^2N,N', respectively. A unique feature of the thermal behavior of the complexes $[Eu_2(bath)_2(piv)_6]\cdot x$Solv upon heating in an inert atmosphere below the decomposition temperature (~320–325°C) of desolvated pivalates $[Eu_2(bath)_2(piv)_6]\cdot x$Solv is they are exhibit phase transitions, namely, the 0D-0D single-crystal-to-single crystal transitions (SCSC), polymorphic transitions, and melting. The thermal behavior upon heating and structural transitions of europium pivalates with the Bath ligand were described in detail [16].

The low-temperature behavior of complex $[Eu_2(Bath)_2(Piv)_6]$ (**I**) was studied by adiabatic calorimetry in a temperature range of 5.96–302.88 K. The temperature dependence of the heat capacity ($C_p^\circ(T)$) for complex **I** is shown in Fig. 1. The standard thermodynamic functions $C_p^\circ(T)$, $S^\circ(T)$, $\Phi^\circ(T) - \Phi^\circ(0)$, and $H^\circ(T) - H^\circ(0)$ of complex **I** were obtained from the experimental adiabatic calorimetry data and are given in Table 3. The $C_p^\circ(T)$ dependence exhibits a monotonic (without sharp changes corresponding to hypothetical phase transitions) decrease in C_p° indicating no phase transitions for complex **I** in the studied temperature range. A similar behavior of the $C_p^\circ(T)$ dependence is demonstrated by complexes $[Ln_2(Phen)_2(Piv)_6]$, where Ln = Sm, Eu, and Tb [18, 19, 28], in the temperature range 5–$T_{\text{Phen removal}}$ (~263°C). It can be confirm that the absence of conjugation between the Ph and Phen fragments of structurally nonrigid ligands Bath in complex **I** induces no thermal changes in the conformation of Bath coordinated on the metal in a temperature range of 5.96–302.88 K. Unlike this, the $C_p^\circ(T)$ dependences in a temperature range of 5–$T_{\text{Bpy removal}}$ (~148°C) of complexes $[Ln_2(Bpy)_2(Piv)_6]$, where Ln = Sm, Eu, Gd, and Er, containing the conformationally labile ligand Bpy exhibit anomalies near 233 K (–40°C) related to thermal changes in the conformation of the Bpy ligand [18, 19, 28]. The absence of structural changes in the temperature range 5–$T_{\text{neutral ligand removal}}$ K for the series of binuclear complexes $[Ln_2L_2(Piv)_6]$ (where Ln = Sm, Eu, Gd, Tb, and Er; L = Bpy or Phen), as well as $[Ln_2(HPiv)_6(Piv)_6]\cdot$HPiv (where Ln = La, Sm, Eu, Gd, and Tb), which are related to defreezing degrees of freedom of the Piv anionic ligands [18, 19, 28, 29], makes it possible to expect a structural stability of the $[Eu_2(Bath)_2(Piv)_6]\cdot x$Solv complexes in a temperature range of 5.96–302.88 K.

We have previously shown that the heterocyclic N-donor ligands Bath, Phen, and Bpy exhibiting intense absorption bands in the near-UV spectral range efficiently sensitize the PL of the Eu^{3+} ion in

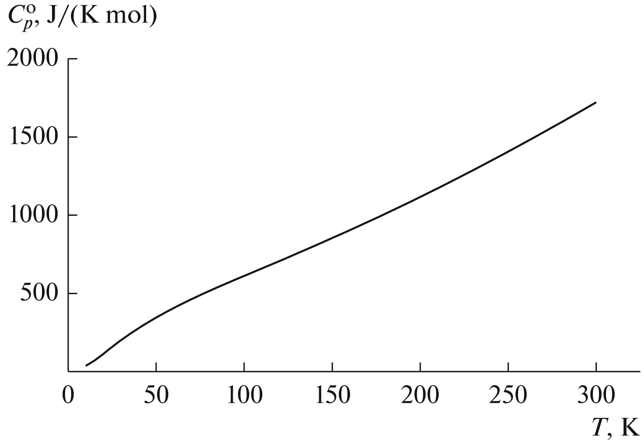

Fig. 1. Temperature dependence of the heat capacity for complex **I**.

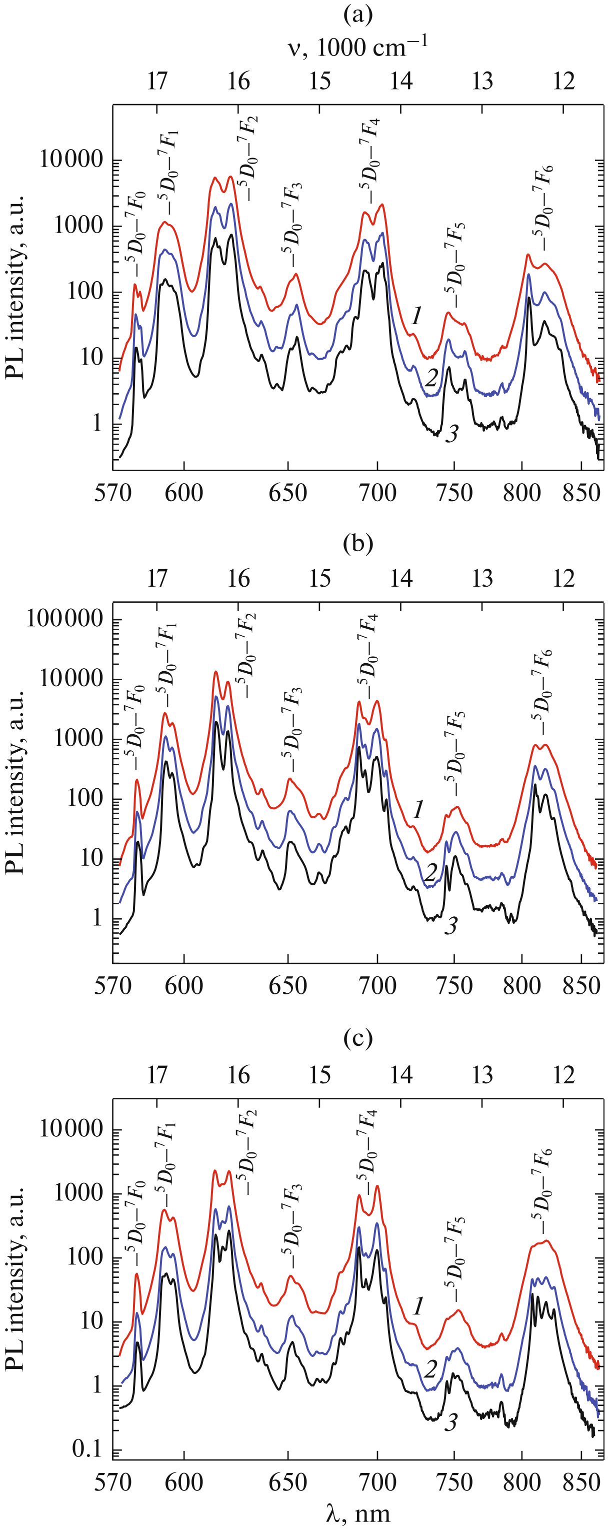

Fig. 2. PL spectra of complexes (a) **I**, (b) **II**, and (c) **III** at 295 ((*1*) multiplied by 9), 193 ((*2*) multiplied by 3), and 98 K (*3*).

binuclear pivalates $[Eu_2(Bath)_2(Piv)_6]\cdot x$Solv, $[Eu_2(Phen)_2$-$(Piv)_6]$ (**II**), and $[Eu_2(Bpy)_2(Piv)_6]$ (**III**) and provide high absolute PL quantum yields (~60%) upon PL excitation in the spectral range corresponding to the ligand absorption [16, 17, 19].

The low-temperature behavior of the integral photoluminescence intensity of the $^5D_0$–^7F_j (j = 0–6) transitions of the Eu^{3+} ion for complexes **I**–**III** was studied by luminescence spectroscopy in a temperature range of 98–295 K. The PL spectra of complexes **I**–**III** at 295, 193, and 98 K are shown in Fig. 2. Upon UV excitation at a wavelength of 340 nm, complexes **I**–**III** demonstrate a bright red luminescence of the Eu^{3+} ion. The spectra of the compounds contain narrow PL bands characteristic of electron transitions of the Eu^{3+} ion from the $^5D_0$ level to the sublevels of the fundamental term ^7F_J (J = 0–6). As the temperature decreases, the spectra of complexes **I**–**III** exhibit a decrease in the width of all spectral lines of the transitions of the Eu^{3+} ion, except the zero-phonon line of the $^5D_0$–$^7F_0$ transition due to a decrease in the interaction of Eu^{3+} ions with phonons of the crystalline lattice [30]. No substantial changes in the Stark structure of PL bands of Eu^{3+} ions are observed in the PL spectra of complexes **I**–**III** at 193 and 98 K as compared to the corresponding PL spectra of these complexes at 295 K. This indicates that the local electric field of the Eu^{3+} ion is retained [31] in a temperature range of 98–295 K in complexes **I** and **II**, as well as in complex **III** for which an anomaly on the $C_p^\circ(T)$ dependence was found near 233 K. The anomaly is related to intrasphere thermal changes in the conformation of the Bpy ligand [28].

We have found that complexes **I** and **II** demonstrate a high temperature stability of the integral PL intensity in a wavelength range of 564–880 nm corresponding to luminescence bands of the $^5D_0$–^7F_j (j = 0–6) transitions of the Eu^{3+} ion in a temperature range of 98–295 K. As the temperature decreases from 295 to 98 K, complexes **I** and **II** demonstrate a monotonic decrease in the integral PL intensity being no more than 7 and 3% for complexes **I** and **II**, respectively. Moreover, as the temperature decreases from 295 to 193 K, the integral PL intensity for complexes **I** and **II** decreases only by 2.4 and 2%, respectively. Note that the change in the absolute PL quantum yield is directly proportional to the change in the PL intensity [32]. Thus, in a temperature range of 98–295 K, complexes **I** and **II** retain high absolute PL quantum yields being at least 55.8 and 58.2%, respectively. The absolute PL quantum yields of complexes **I** and **II** in a temperature range of 193–295 K (from –80 to +22°C) are at least 58.6 and 58.8%, respectively. The proximity of the corresponding energy values of the S1 and T_1 states of the Bath ligand for variety of complexes $[Gd_2(Bath)_2(Piv)_6]\cdot x$Solv [17] allow one to expect close absolute quantum yields for variety of complexes $[Eu_2(Bath)_2(Piv)_6]\cdot x$Solv in a temperature range of 295–98 K. Note that on decreasing temperature from 295 to 98 K the lifetime of the $^5D_0$ level of the Eu^{3+} ion increases by 29 and 3.7% for complexes **I** and **II**, respectively. Since no corresponding increase in the PL intensity is observed for pivalates **I** (29%) and **II** (3.7%) with decreasing temperature from 295 to 98 K, it can be assumed that the channel of ligand–metal excitation energy transfer is deactivated along with the quenching channel of the $^5D_0$ level of the Eu^{3+} ion (by 6.7 and 36%, respectively) with the temperature decrease for complexes **I** and **II**, which compensates the temperature effect on the PL intensity in a temperature range of 295–98 K. That is, despite the fact that the fraction of radiative relaxation of the $^5D_0$ level to the ^7F_j (j = 0–6) levels increases with the temperature decrease, the $^5D_0$ level is populated with a lower probability with the temperature decrease. For complex **III** with decreasing temperature from 295 to 193 K, a monotonic decrease in the integral PL intensity by 30% is observed, and then some increase is observed with the further temperature decrease to 98 K. The total change in the intensity in a range of 295–98 K is 25%. Thus, in the temperature range from 98 to 295 K, the absolute PL quantum yield of the complex is at least 41%. Taking into account that with decreasing temperature from 295 to 98 K the lifetime of the $^5D_0$ level increases by 4%, we can assume that the channel of ligand–metal excitation energy transfer undergoes deactivation by at least 29% in a temperature range of 295–98 K. This deactivation explains a decrease in the PL intensity in a temperature range of 295–193 K. The deactivation of the quenching channel of the $^5D_0$ level becomes appreciable in a temperature range of 193–98 K where the PL intensity decrease changes by an increase when the temperature decreases.

To conclude, the absence of low-temperature phase transitions in a temperature range of 5.96–302.88 K was shown, and the most important thermodynamic functions $C_p^\circ(T)$, $S^\circ(T)$, $\Phi^\circ(T)$, and $H^\circ(T) - H^\circ(0)$ were calculated for complex **I**. In a temperature range of 98–295 K, complexes **I**–**III** retain high absolute quantum PL yields being at least 55.8, 58.2, and 41% for complexes **I**–**III**, respectively. The absolute PL quantum yields of complexes **I** and **II** in a temperature range of 193–295 K (from –80 to +22°C) are at least 58.6 and 58.8%, respectively. An insignificant decrease in the integral PL intensity corresponding to the luminescence bands of the $^5D_0$–^7F_j (j = 0–6) transitions of the Eu^{3+} ion with decreasing temperature for complexes **I**–**III** is due to the mutual compensation of the temperature activation of the channels of ligand–metal excitation transfer and channels of nonradiative excitation relaxation for these complexes. The results obtained in this work (in combination with the results of our studies of the photophysical properties and thermal behavior of the binuclear europium pivalates in a temperature range of 30–600°C [16, 18, 19]) showing the thermal stability of the complexes, a significant monochromaticity, and high absolute PL quantum yields of the binuclear europium pivalates with ligands Bath, Phen, and Bpy, as well as a high volatility of the binuclear lanthanide pivalates [10, 13–15, 33–36]) indicate that complexes $[Eu_2(Bath)_2(Piv)_6]\cdot x$Solv, **II**, and **III** are promising functional components of new luminescent materials in a temperature range of 98–295 K.

ACKNOWLEDGMENTS

This work was supported by the Ministry of Science and Higher Education of the Russian Federation as part of the State Assignment of the Kurnakov Institute of General and Inorganic Chemistry of the Russian Academy of Sciences. This research was performed using the equipment of the JRC PMR IGIC RAS.

FUNDING

This work was supported by the Ministry of Science and Higher Education of the Russian Federation as a part of the state assignment of the Kurnakov Institute of General and Inorganic Chemistry Russian Academy of Sciences.

CONFLICT OF INTEREST

The authors of this work declare that they have no conflicts of interest.

REFERENCES

1. Huang, C.-H., *Rare Earth Coordination Chemistry: Fundamentals and Applications*, Singapore: Wiley, 2010.
2. Binnemans, K., in *Handbook on the Physics and Chemistry of Rare Earths*, Gschneidner, K.A., Jr., Bünzli, J.-C.G, and Pecharsky, V.K., Eds., Amsterdam: Elsevier, 2005, vol. 35, p. 107.

3. Gatteschi, D., Sessoli, R., and Villain, J., *Molecular Nanomagnets*, Oxford: Oxford University, 2006.
4. *Metal Ions in Biological Systems: The Lanthanides and Their Interrelations with Biosystems*, Sigel, H. and Sigel, A., Eds., Basel: Marcel Dekker, 2003, vol. 40.
5. Lan, Y.-Q., Jiang, H.-L., Li, S.-L., et al., *Inorg. Chem.*, 2012, vol. 51, p. 7484.
6. Zhu, Y., Luo, F., Luo, M., et al., *Dalton Trans.*, 2013, vol. 42, p. 8545.
7. Bunzli, J.-C.G., Chauvin, A.-S., Kim, H.K., et al., *Coord. Chem. Rev.*, 2010, vol. 254, p. 2623.
8. Shavaleev, N.M., Scopelliti, R., Gumy, F., et al., *Inorg. Chem.*, 2009, vol. 48, p. 6178.
9. Shavaleev, N.M., Gumy, F., Scopelliti, R., et al., *Inorg. Chem.*, 2009, vol. 48, p. 5611.
10. Fomina, I.G., Dobrokhotova, Zh.V., Ilyukhin, A.B., et al., *Polyhedron*, 2013, vol. 65, p. 152.
11. Law, G.-L., Kwok, W.-M., Wong, W.-T., et al., *J. Phys. Chem. B*, 2007, vol. 111, p. 10858.
12. Brito, H.F., Malta, O.L., Felinto, M.C.F.C., and Teotonio, E.E.S., *The Chemistry of Metal Enolates*, Zabicky, J., Ed., Wiley 2009, Ch. 3, p. 131.
13. Fomina, I.G., Dobrokhotova, Zh.V., Aleksandrov, G.G., et al., *Polyhedron*, 2013, vol. 50, p. 297.
14. Fomina, I.G., Dobrokhotova, Zh.V., Ilyukhin, A.B., et al., *Dalton Trans.*, 2014, vol. 43, p. 18104.
15. Fomina, I.G., Dobrokhotova, Zh.V., Ilyukhin, A.B., et al., *Russ. Chem. Bull.*, 2014, vol. 63, no. 4, p. 938. https://doi.org/10.1007/s11172-014-0531-9
16. Fomina, I.G., Ilyukhin, A.B., Zavorotny, Y.S., et al., *Polyhedron*, 2017, vol. 129, p. 105.
17. Fomina, I.G., Dolgushin, F.M., Koroteev, P.S., et al., *Eur. J. Inorg. Chem.*, 2021, vol. 2021, no. 5, p. 464.
18. Dobrokhotova, Zh.V., Fomina, I.G., Aleksandrov, G.G., et al., *Russ. J. Inorg. Chem.*, 2009, vol. 5, p. 668. https://doi.org/10.1134/S0036023609050040
19. Fomina, I.G., Dobrokhotova, Zh.V., Kazak, V.O., et al., *Eur. J. Inorg. Chem.*, 2012, vol. 22, p. 3595.
20. Malyshev, V.M., Mil'ner, G.A., Sorkin, E.L., et al., *Pribory i tekhnika eksperimenta*, 1985, no. 6, p. 195.
21. Varushchenko, R.M., Druzhinina, A.I., and Sorkin, E.L., *J. Chem. Thermodyn.*, 1997, vol. 29, no. 6, p. 623.
22. Gurevich, V.M. and Khluystov, V.G., *Geokhimiya*, 1979, vol. 17, no. 6, p. 829.
23. NIST ITS-90 Thermocouple Database. https://doi.org/10.18434/T4S888
24. Gurvich, A.M., *Vvedenie v fizicheskuyu khimiyu kristallofosforov. Ucheb. posobie dlya vtuzov* (Introduction to Physical Chemistry of Crystal Phosphors. Study Book for Higher Technical Colleges), Moscow: Vyssh. shkola, 1971, p. 40.
25. Carnall, W.T. and Crosswhite, H.M., *Argonne Natl. Lab. Rept.*, 1977, p. ANL78XX95.
26. Fomina, I.G., Kiskin, M.A, Martynov, A.G., et al., *Russ. J. Inorg. Chem.*, 2004, vol. 49, p. 1349.
27. Fomina, I.G., Ilyukhin, A.B., Gavrikov, A.V., et al., *Inorg. Chim. Acta*, 2018, vol. 482, p. 8.
28. Dobrokhotova, Zh.V., Tyurin, A.V., Fomina, I.G., et al., *Thermochim. Acta*, 2013, vol. 556, p. 68.
29. Dobrokhotova, Zh.V., Fomina, I.G., Kiskin, M.A., et al., *Russ. J. Phys. Chem.*, 2006, vol. 3, p. 323. https://doi.org/10.1134/S0036024406030034
30. Osad'ko, I.S., *Phys. Rep.*, 1991, vol. 206, no. 2, p. 43.
31. Zolin, V.F., Koreneva, L.G. *Redkozemel'nyi zond v khimii i biologii* (Rare Earth Probe in Chemistry and Biology), Moscow: Nauka, 1980, p. 350.
32. Zolotov, Yu.A. *Osnovy analiticheskoi khimii* (Fundamentals of Analytical Chemistry), Moscow: Akademiya, 2012, vol. 2.
33. Fomina, I.G., Dobrokhotova, Zh.V., Aleksandrov, G.G., et al., *J. Solid State Chem.*, 2012, vol. 185, p. 49.
34. Malkerova, I.P., Alikhanyan, A.S., Fomina, I.G., et al., *Russ. J. Inorg. Chem.*, 2009, vol. 54, no. 5, p. 734. https://doi.org/10.1134/S0036023609050118
35. Malkerova, I.P., Alikhanyan, A.S., Fomina, I.G., et al., *Russ. J. Inorg. Chem.*, 2010, vol. 55, no. 1, p. 53. https://doi.org/10.1134/S0036023610010109
36. Emelina, A.L., Dobrokhotova, Zh.V., Sinelshchikova, A.A., et al., *Russ. J. Inorg. Chem.*, 2009, vol. 55, no. 11, p. 1754. https://doi.org/10.1134/S0036023610110124

Translated by E. Yablonskaya

Publisher's Note. Pleiades Publishing remains neutral with regard to jurisdictional claims in published maps and institutional affiliations.